Comparisons of Two Ensemble Mean Methods in Measuring the Average Error Growth and the Predictability*

DING Ruiqiang†(丁瑞强) and LI Jianping (李建平)

State Key Laboratory of Numerical Modeling for Atmospheric Sciences and Geophysical Fluid Dynamics (LASG), Institute of Atmospheric Physics, Chinese Academy of Sciences, Beijing 100029

(Received April 6, 2010; in final form March 21, 2011)

ABSTRACT

In this paper, taking the Lorenz system as an example, we compare the influences of the arithmetic mean and the geometric mean on measuring the global and local average error growth. The results show that the geometric mean error (GME) has a smoother growth than the arithmetic mean error (AME) for the global average error growth, and the GME is directly related to the maximal Lyapunov exponent, but the AME is not, as already noted by Krishnamurthy in 1993. Besides these, the GME is shown to be more appropriate than the AME in measuring the mean error growth in terms of the probability distribution of errors. The physical meanings of the saturation levels of the AME and the GME are also shown to be different. However, there is no obvious difference between the local average error growth with the arithmetic mean and the geometric mean, indicating that the choices of the AME or the GME have no influence on the measure of local average predictability.

Key words: predictability, arithmetic mean, geometric mean, Lorenz system

Citation: Ding Ruiqiang and Li Jianping, 2011: Comparisons of two ensemble mean methods in measuring the average error growth and the predictability. *Acta Meteor. Sinica*, **25**(4), 395–404, doi:10.1007/s13351-011-0401-4.

1. Introduction

The atmosphere is a forced dissipative nonlinear system. On the assumption that external forces are bounded, the existence of the atmosphere attractor has been mathematically proved (Li and Chou, 1997; Li and Wang, 2008). The predictability of atmospheric weather fluctuations is limited to 1–2 weeks due to the nonlinearity and instability properties of the atmospheric flow (Lorenz, 1963, 1969; Zhou, 2005). Up to now, the predictability studies of the atmosphere are mainly based on numerical models (Leith, 1983; Simmons et al., 1995; Mu et al., 2002; Lang and Wang, 2005). If the solutions evolving from several initial states closely located around an assumed true state have been obtained, the divergence of all the solutions from the true solution is then determined. The predictability of the model is expressed in terms of the growth rate of the root mean square (RMS) error and the doubling time of small errors.

Atmospheric predictability is found to vary obviously with time and it depends on the particular state of atmospheric flow patterns (Lorenz, 1965; Legras and Ghil, 1985; Yoden and Nomura, 1993; Ding et al., 2008a). To understand the average predictability properties of the atmosphere, an ensemble mean of error growth at different initial states must be considered. The ensemble mean can be either arithmetic or geometric. In previous studies, the arithmetic mean is widely used to measure the average growth of the errors, as in the ensemble prediction systems (Tracton and Kalnay, 1993; Palmer et al., 1993). However, the arithmetic mean is found to have a weakness. If one or two values of the errors are either extremely large or extremely small compared to the majority of the errors, the arithmetic mean might not be an appropriate average to represent the errors. In that case the geometric mean can better represent the average

*Supported by the National Natural Science Foundation of China (40805022 and 40675046) and the National Basic Research and Development (973) Program of China (2010CB950400).

†Corresponding author: drq@mail.iap.ac.cn.

errors. The geometric mean was applied in several recent studies, showing good properties. For example, the amplitude factor as the spatial geometrical mean value of a perturbation, as introduced by López et al. (2004), is directly related to the maximal Lyapunov exponent and exhibits nice scaling properties. A new ensemble method (logarithmic bred vectors) based on the geometric mean of the perturbations, as presented by Primo et al. (2008), increases the diversity of the ensemble and allows the spread to grow faster.

Since the error growth with the arithmetic mean is different from that with the geometric mean, the estimated predictability based on the error growth is also different. Based on the Lorenz's 28-variable model, Krishnamurthy (1993) compared the differences between the error growth with the arithmetic mean and the error growth with the geometric mean, and found that the RMS error shows a smoother growth when the computed mean is geometric rather than arithmetic. Except the work of Krishnamurthy (1993), few studies have been performed to investigate the influences of ensemble mean methods of errors on the predictability measurement. To further understand which method should be chosen to better measure the predictability, it is necessary to investigate again the differences between two kinds of ensemble mean methods in describing the error growth. In this paper, taking the Lorenz system as an example, we further compare the differences between two kinds of ensemble mean methods in measuring the predictability. The results show that the geometric mean error (GME) shows a smoother growth than the arithmetic mean error (AME) for the global average error growth, and that the GME is directly related to the maximal Lyapunov exponent, but the AME is not. These findings are consistent with Krishnamurthy (1993). In addition, we show that the GME is more appropriate than the AME in measuring the mean error growth in terms of the probability distribution of errors. We also show the physical meanings of the saturation levels of the AME and the GME. There is no obvious difference between the local average error growth with the arithmetic mean and the geometric mean, which is also a major finding of this work.

2. Global average growth of errors

Let $x_1, x_2, x_3, \cdots, x_n$ be n positive numbers. Their arithmetic mean and geometric mean are written as $(x_1+x_2+\cdots+x_n)/n$ and $\sqrt[n]{x_1x_2\cdots x_n}$, respectively. It is easy to prove the following inequality,

$$\sqrt[n]{x_1x_2\cdots x_n} \leqslant \frac{x_1+x_2+\cdots+x_n}{n}, \tag{1}$$

where the equality sign holds only when $x_1 = x_2 = \cdots = x_n$. The Lorenz system is

$$\begin{cases} \dot{X} = -\sigma X + \sigma Y, \\ \dot{Y} = rX - Y - XZ, \\ \dot{Z} = XY - bZ, \end{cases} \tag{2}$$

where $\sigma = 10$, $r = 28$, and $b = 8/3$, for which the well-known "butterfly" attractor exists (Lorenz, 1963). From a long integration by using the fourth order Runge-Kutta method with a time stepsize $h = 0.01$, 1×10^4 points are obtained within the attractor to form an ensemble of initial unperturbed states. Then an initial error is superimposed on the unperturbed states to form an ensemble of perturbed states. By integrating the Lorenz system, the solutions originating from the unperturbed and perturbed initial states are determined to obtain an ensemble of 1×10^4 errors at each time step. For notational simplicity, let the norm of error in phase space at time τ be $\delta(\tau) = \|\delta(\tau)\|$. For chaotic systems, $\delta(\tau)$ is always positive. The ensemble mean of the growth of errors over n initial states is given as

$$\overline{\delta}(\tau) = \langle \delta(\boldsymbol{x}_i, \tau) \rangle_n, \tag{3}$$

where $\langle\ \ \rangle_n$ denotes the ensemble average of errors over n initial states ($n = 1\times10^4$), $\delta(\boldsymbol{x}_i, \tau)$ (hereafter, for simplicity denoted as $\delta_i(\tau)$) denotes the error magnitude at the initial state $\boldsymbol{x}_i$ ($i = 1, 2, \cdots, n$), and τ is the evolution time. The ensemble mean can be defined as the arithmetic or geometric over all n ensemble members.

The ensemble mean of the growth of errors with initial magnitude $\delta_0 = 10^{-6}$ is presented in Fig. 1. The two error curves represent the arithmetic mean and the geometric mean of the error growth,

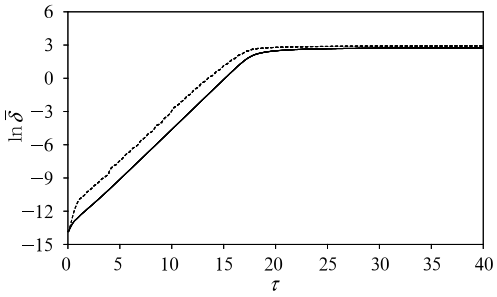

Fig. 1. Evolution of the AME (dashed line) and the GME (solid line) with time. The magnitude of initial error is 10^{-6}.

respectively. The error shows a smoother growth when the computed mean is geometric rather than arithmetic, consistent with Krishnamurthy (1993). In a very short time interval, there are only trivial differences between the AME and the GME. With the time increasing, the AME begins to depart from the GME. In accordance with the inequality Eq. (1), the AME is significantly greater than the GME for most of the time. Both the AME and the GME finally stop increasing and reach the saturation level.

For the initial errors with the same magnitude $\delta_0 = 10^{-6}$, superimposed on the 1×10^4 initial states, they will gradually diverge as time goes by. From the distributions of the errors $\delta_i(\tau)$, the histograms seem to concentrate on few bars because most of the errors are really small compared to a few big values for different times τ = 1, 4, 7, and 10 (Figs. 2a–d). If making the logarithmic transform of the errors $\delta_i(\tau)$, we found that the resultant $\ln(\delta_i(\tau))$ shows a character of normal distribution (Figs. 2f–i). Similar results have been found by Primo et al. (2008) and Gutiérrez et al. (2008), who pointed out that the spatial finite perturbations in spatiotemporal chaos follow a lognormal distribution and that they become Gaussian after a logarithmic transform. As a result, the Gaussian techniques become feasible. The new parameters introduced by them are exactly based on this property of the perturbations. Since $\ln(\delta_i(\tau))$ can be characterized in terms of normal distributions, its mean represents the most probable one. The mean of $\ln(\delta_i(\tau))$ is just the logarithmic of the geometric mean of the errors $\delta_i(\tau)$; consequently, the GME primarily represents the average of the most probable errors. On the contrary, the mean of the errors $\delta_i(\tau)$, i.e., the AME, mainly reveals the average of the errors with large magnitudes, which commonly have little probability to occur (Figs. 2a–e).

In addition, it is noted from Fig. 3 that the growth of the GME is almost perfectly exponential during much of the growth phase before saturation, with a growth rate consistent with the maximal Lyapunov exponent of Lorenz system. The results show that the GME is directly related to the maximal Lyapunov exponent, consistent with López et al. (2004). The maximal Lyapunov exponent is defined as the long-term average growth rate of an infinitesimal initial error (Wolf et al., 1985; Eckmann and Ruelle, 1985):

$$\lambda_1 = \lim_{\tau\to\infty}\lim_{\delta(0)\to0}\frac{1}{\tau}\ln\frac{\delta(\tau)}{\delta(0)}, \tag{4}$$

where $\delta(0)$ is the norm of an infinitesimal initial error superimposed at the initial state $\boldsymbol{x}$, and $\delta(\tau)$ denotes the final separation distance of the infinitesimal initial error. In the calculation of the maximal Lyapunov exponent, the average of local growth rates of initially small errors is generally served as one of its approximations (Wolf et al., 1985; Nese, 1989; Ziehmann et al., 2000):

$$\lambda_1 \approx \frac{1}{n}\sum_{i=1}^{n}\frac{1}{\tau}\ln\frac{\delta_i(\tau)}{\delta_i(0)}, \qquad (n\to\infty), \tag{5}$$

where $\delta_i(0)$ is a very small initial error superimposed at the initial state $\boldsymbol{x}_i$, and $\delta_i(\tau)$ denotes the error growth during a short time interval τ. For Eq. (5), we have

$$\lambda_1 \approx \frac{1}{\tau}\ln\frac{\sqrt[n]{\delta_1(\tau)\delta_2(\tau)\cdots\delta_n(\tau)}}{\sqrt[n]{\delta_1(0)\delta_2(0)\cdots\delta_n(0)}}. \tag{6}$$

For the same initial error $\delta(0)$, we obtain

$$\sqrt[n]{\delta_1(\tau)\delta_2(\tau)\cdots\delta_n(\tau)} \approx \delta(0)\exp(\lambda_1\tau). \tag{7}$$

Therefore, the maximal Lyapunov exponent describes the exponential growth rate of the GME, unrelated to the AME, suggesting that the growth of errors with geometric mean is more appropriate than with the arithmetic mean as the Lyapunov exponent is

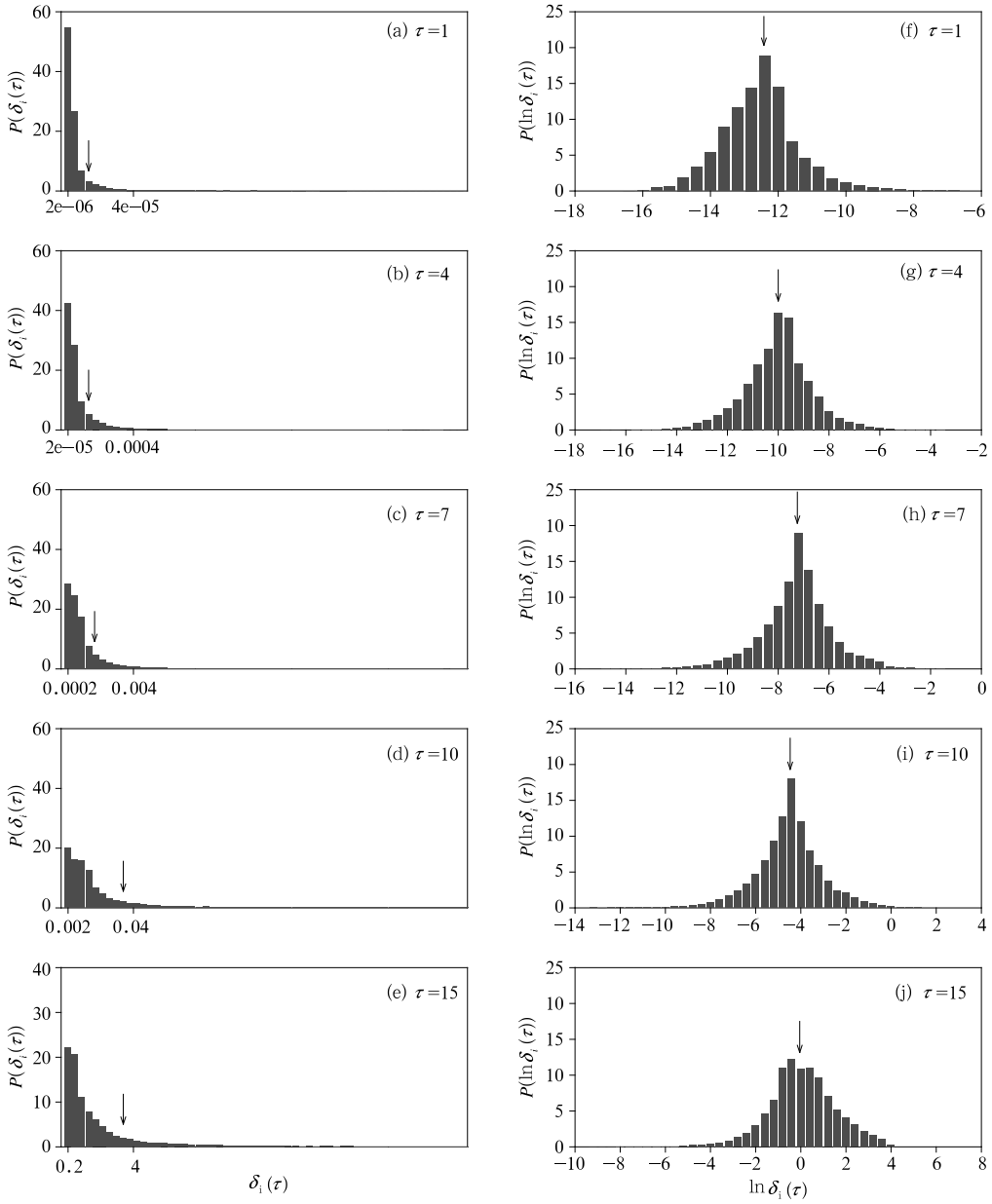

Fig. 2. Left-hand panels show the probability distributions of the error magnitude $\delta_i(\tau)$ ($i = 1,\cdots,1\times10^4$) for different values of time τ (from 1 to 15). Right-hand panels show the corresponding probability distributions of the logarithmic fluctuation values $\ln(\delta_i(\tau))$. The arrows in (a)–(e) indicate the arithmetic mean of the errors $\delta_i(\tau)$, while the arrows in (f)–(j) indicate the arithmetic mean of the logarithmic values $\ln(\delta_i(\tau))$. In (a)–(j), P denotes the probability (%).

simply the average of growth rate of small errors.

Figure 4 shows the growth rates of the AME and the GME, respectively. The growth rate is defined as $\alpha_e = \frac{1}{h}\ln\frac{\overline{\delta}(ih)}{\overline{\delta}((i-1)h)}$, where the time step size $h = 0.01$ and the initial magnitude of errors $\delta_0 = 10^{-6}$. In Fig. 4b, the GME actually decays in a very short time initially before entering the growth phase that progresses at a rate faster than the maximal Lyapunov exponent until $\tau = 2$. Afterwards, the GME enters the exponential growth phase, with the growth rate $\alpha_e \approx \lambda_1$. Finally, the growth of error enters the

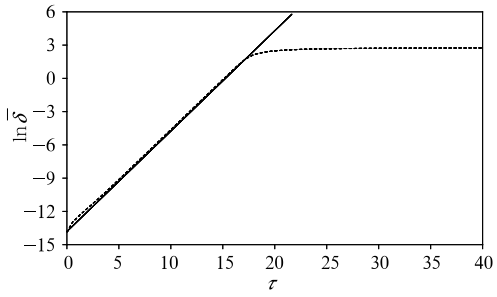

Fig. 3. Exponential growth of errors with the initial magnitude $\delta_0 = 10^{-6}$ and the growth rate $\lambda_1 = 0.905$. λ_1 is the maximal Lyapunov exponent of Lorenz system. The dashed curve represents the GME of Fig. 1.

nonlinear phase with a steadily decreasing growth rate, and the growth rate α_e gradually converges to 0. The results indicate that the geometric mean can clearly describe the process from initially exponential growth to finally enter the nonlinear growth phase for sufficiently small errors. López et al. (2004) found that an initial perturbation of finite size ε_0 grows in time obeying the tangent space dynamics equations up to a characteristic time $t_x(\varepsilon_0) \sim b - (1/\lambda_1)\ln(\varepsilon_0)$, where λ_1 is the maximal Lyapunov exponent and b is a constant. Actually, this characteristic time $t_x(\varepsilon_0)$ is the time before the GME enters the nonlinear phase in Fig. 4b. The behavior of the AME is similar to that of the GME at first, with a very large growth rate after the initial decaying. After that, the growth rate of the AME largely fluctuates around the maximal Lyapunov exponent. The greatest amplitude of the fluctuation is above 1.0. With the time passing, the growth rate of the AME begins to decrease and the fluctuation also weakens. Finally, the growth rate of the AME tends to reach 0 (Fig. 4a).

In previous predictability studies, the growth rate of the errors and the doubling time of small errors are often used to measure the predictability (Lorenz, 1965, 1982). Given that the growth rate of the AME shows a large fluctuation around the maximal Lyapunov exponent, there would be a great uncertainty in the estimate of the predictability. It is possible that the predictability obtained by using the arithmetic mean is lower or higher than that obtained by using the geometric mean, which depends on the time for comparison. From this perspective, it is more appropriate to measure the predictability with the geometric mean than with the arithmetic mean. For chaotic systems, once the error growth reaches the saturation level, almost all information on initial states is lost and the prediction becomes meaningless. Recent studies have defined the time when error growth reaches saturation as the limit of predictability (Dalcher and Kalnay, 1987; Ding and Li, 2007). The time at which error growth reaches saturation only depends on the dynamical characteristic of chaotic systems rather than the ensemble mean methods of errors. Therefore, if taking the saturation time as the measure of predictability, the limit of predictability obtained by using the arithmetic mean is nearly equal to that obtained by using the geometric mean. According to Fig. 1, we determine the limit of the predictability of Lorenz system with the initial error $\delta_0 = 10^{-6}$ as approximately $t_p = 20.0$.

Although both the AME and the GME finally reach saturation, the physical meanings of their saturation levels are different. Over the Lorenz attractor,

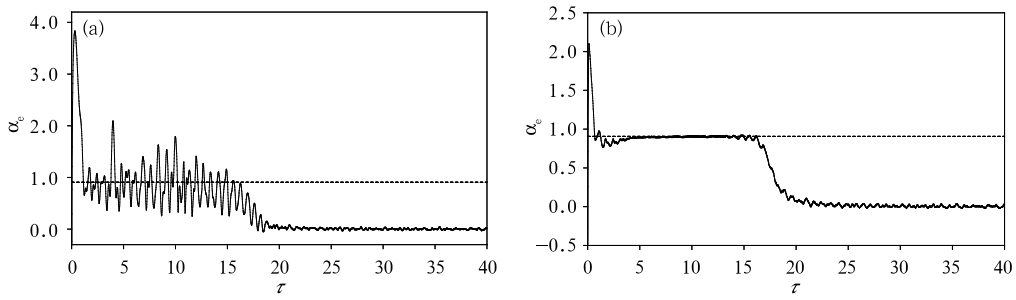

Fig. 4. Growth rates (α_e) of the (a) AME and (b) GME. The initial magnitude of errors is 10^{-6}. The dashed lines indicate the maximal Lyapunov exponent of Lorenz system $\lambda_1 = 0.905$.

two points are randomly chosen and the RMS distance between the two randomly-chosen points is then computed. This process is repeated 10000 times and the average RMS distance $\overline{d}$ between two randomly-chosen points over the Lorenz attractor can finally be obtained. It is found that $\overline{d}$ is identical with the saturation level of the AME (Fig. 5a), implying that the saturation level of the AME represents the average RMS distance between two randomly-chosen points over the attractor. The saturation level of the GME can be proven to be related to the probability distribution of errors over the Lorenz attractor (Ding and Li, 2007), and it can be obtained by the probability distribution of errors. Next, we give a theorem and then present the proof of the theorem.

The relationship between the saturation level of the GME and the probability distribution of errors can be inferred from this theorem.

Main theorem: Assume that the independent random variables $X_1, X_2, \cdots\cdots, X_n$ have the following probability distribution:

$$f(x) = \begin{cases} p(x), & \varepsilon \leqslant x \leqslant a, \\ 0, & x < \varepsilon \text{ or } x > a, \end{cases} \tag{8}$$

where ε is an arbitrary small positive number, a is a positive constant, and $p(x)$ is a continuous function defined on a closed interval $[\varepsilon, a]$. Let $Z_n = \Big(\prod_{i=1}^{n} X_i\Big)^{1/n}$, then

$$Z_n \xrightarrow{p} c, \qquad (n \to \infty), \tag{9}$$

where $\xrightarrow{p}$ denotes the convergence in probability (Rose and Smith, 2002) and c is a constant depending on $p(x)$.

A concise proof of the theorem can be given as follows. Firstly we have

$$\ln Z_n = \frac{1}{n}\sum_{i=1}^{n} \ln X_i.$$

Since X_i $(i = 1, 2, \cdots, n)$ follows an independent identical distribution, so does $\ln X_i$ $(i = 1, 2, \cdots, n)$, the mathematical expectation follows that

$$E(\ln X_i) = \int_{\varepsilon}^{a} \ln x \cdot p(x)\mathrm{d}x = b,$$

where b is a constant that depends on $p(x)$. Using the Khinchine's Weak Law of Large Numbers, as $n \to \infty$, we obtain

$$\ln Z_n \xrightarrow{p} b.$$

Then we have $Z_n \xrightarrow{p} \mathrm{e}^b = c$. The proof of our main theorem is completed.

For chaotic systems, as $\tau \to \infty$, $\delta_1(\tau)$, $\delta_2(\tau)$, $\cdots\cdots$, $\delta_n(\tau)$ will follow an independent identical distribution similar to Eq. (8) (Ding and Li, 2007) (because the chaotic attractor is confined to a finite region, a is thought to be the maximum value of $\delta_i(\tau)$ and ε is the minimum value of $\delta_i(\tau)$). Consequently, all conditions of the main theorem are satisfied, and then we obtain

$$\sqrt[n]{\delta_1(\tau)\delta_2(\tau)\cdots\delta_n(\tau)} \xrightarrow{p} c, \qquad (n \to \infty),$$

where c can be considered as the theoretical saturation level of the GME. Using the converged probability distribution of errors over the attractor, the theoretical saturation level of the GME can be determined. From Fig. 5b, the theoretical saturation level of the GME

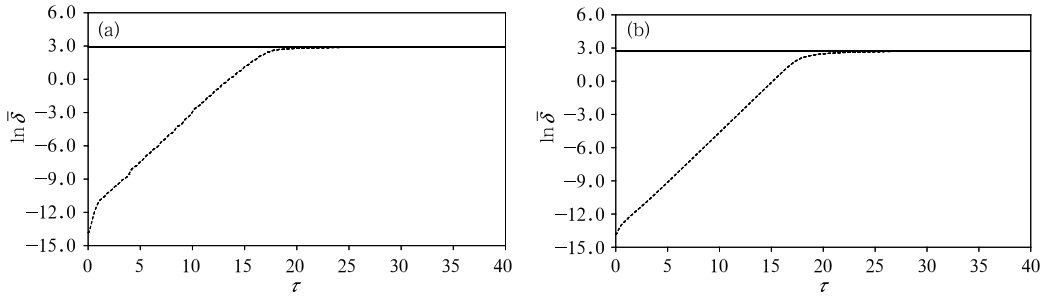

Fig. 5. (a) The average distance between two points that are randomly chosen over the Lorenz attractor and (b) the theoretical saturation level of the GME calculated by the converged probability distribution of errors over the Lorenz attractor. The dashed curves represent the AME and the GME of Fig. 1, respectively.

is found to be completely in line with the actual one. Two initially close points over the chaotic attractor will separate with time and finally become unrelated. At that moment the probability distribution of the RMS error between two unrelated points will converge to an independent identical distribution, which determines the saturation level of the GME. The saturation level of the AME represents the average RMS error between two unrelated points over the attractor. From this point of view, the saturation level of the GME is closely connected with that of the AME, and they both reflect a total loss of initial information for chaotic systems.

Figure 6 shows the dependence of the AME and the GME on the magnitude of the initial error. Regardless of the magnitude of the initial error δ_0, the AME and the GME both finally stop increasing and reach the saturation level. The time at which the AME and the GME reach saturation also lengthens as δ_0 is reduced. Similar to the case for $\delta_0 = 10^{-6}$, there are only trivial differences between the AME and the GME at the beginning, but the AME is significantly greater than the GME with the time increasing. The growth rates of the GME with $\delta_0 = 10^{-9}$ (Fig. 7b) and $\delta_0 = 10^{-1}$ (Fig. 8b) are similar to those with $\delta_0 = 10^{-6}$ (Fig. 4); however, the duration of the exponential growth phase (with the growth rate equal to the maximal Lyapunov exponent) of the GME lengthens as δ_0 becomes smaller and shortens as δ_0 becomes larger. When the magnitude of the initial error nears 1.0, the exponential growth phase of the GME will disappear and the error growth will directly enter the nonlinear phase (figure omitted). The time taken for the AME to fluctuate around the maximal Lyapunov exponent also increases as δ_0 becomes smaller

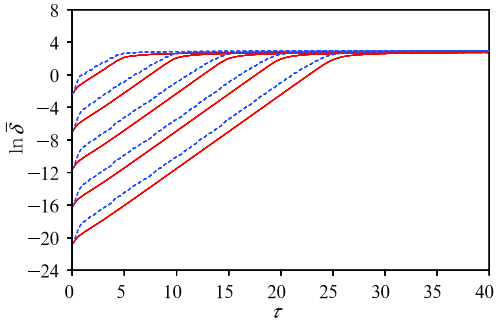

Fig. 6. Evolution of the AME (dashed line) and the GME (solid line) with time for δ_0 of various magnitudes. From top to bottom, the dashed (or solid) curves correspond to $\delta_0 = 10^{-9}$, 10^{-7}, 10^{-5}, 10^{-2}, and 10^{-1}, respectively.

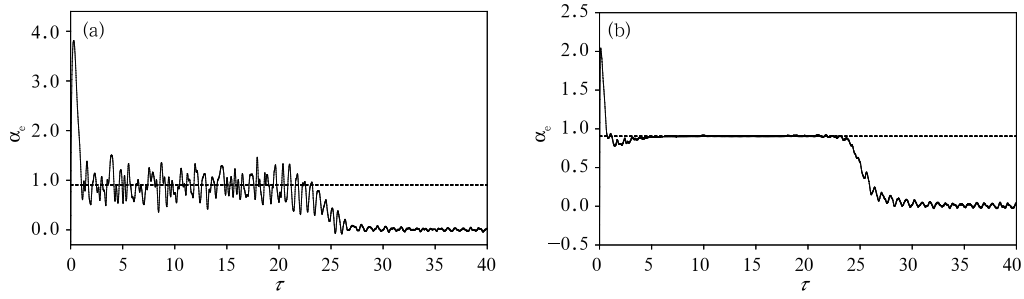

Fig. 7. As in Fig. 4, but the magnitude of initial error is 10^{-9}.

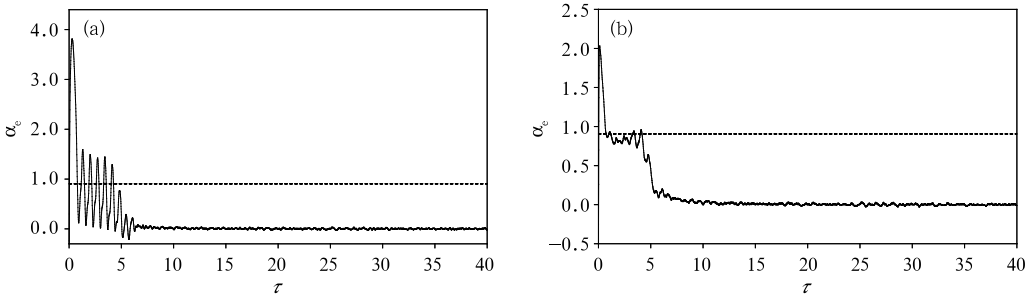

Fig. 8. As in Fig. 4, but the magnitude of initial error is 10^{-1}.

(Fig. 7a) and decreases as δ_0 becomes larger (Fig. 8a).

3. Local average growth of errors

For the Lorenz system, assuming that all initial perturbations with the amplitude ε and random directions are on a three-dimensional spherical surface centered at an initial point $\boldsymbol{x}_0$,

$$\boldsymbol{\delta}_0^{\mathrm{T}}\boldsymbol{\delta}_0 = \varepsilon^2. \tag{10}$$

The local ensemble mean of the growth of errors over a large number of random initial perturbations is given by

$$\overline{\delta}(\tau) = \langle \delta_i(\boldsymbol{x}_0, \tau)\rangle_n, \tag{11}$$

where $\langle\ \rangle_n$ denotes the ensemble average of errors over n initial random errors ($n = 1\times10^4$), and $\delta_i(\boldsymbol{x}_0, \tau)$ denotes the growth of initial random error δ_{0i} (i = 1, 2, $\cdots, n$) at the initial state $\boldsymbol{x}_0$. Same to the global ensemble average, the local ensemble average can also be taken to the arithmetic mean or the geometric mean over all n ensemble members. Figure 9 shows the average growth of errors introduced at the initial state $\boldsymbol{x}_{01}$(10.25, 6.33, 33.33). The initial magnitude of random errors is 10^{-6}. A remarkable feature of Fig. 9 is that, regardless of the arithmetic mean or the geometric mean, two error curves display nearly same behavior in their instantaneous growth or decay starting from the initial time. Finally, the two error curves stop growing and enter the nonlinear stochastic fluctuation states. At that moment almost all information on initial states is lost and the prediction becomes meaningless. If the limit of local predictability is defined as the time at which error reaches the average value of nonlinear stochastic fluctuation states (Ding et al., 2008b), the predictability limit of the system at $\boldsymbol{x}_{01}$ can be quantitatively determined as $t_p = 18.4$. For the other initial state over the Lorenz attractor $\boldsymbol{x}_{02}$(–7.28, –12.06, 16.15), the AME and the GME also show consistent evolutions with time (Fig. 10). These results can be explained by the fact that the error dynamics is dependent on the local dynamics of the unperturbed trajectory starting from the initial state $\boldsymbol{x}_0$ (Fig. 11). The n random errors with the same magnitude but different directions will be rapidly aligned toward the most rapidly growing perturbation along the unperturbed trajectory, causing the magnitudes of n random errors nearly equal. Therefore, the AME and the GME are almost equal for different times. It is indicated that there is no obvious difference between the local average error growth with the arithmetic mean and the geometric mean.

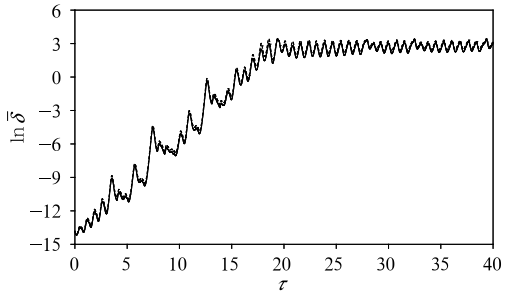

Fig. 9. Growth of the arithmetic mean (dashed line) and the geometric mean (solid line) of random errors introduced at the initial state $\boldsymbol{x}_{01}$(10.25, 6.33, 33.33). The initial magnitude of random errors is 10^{-6}.

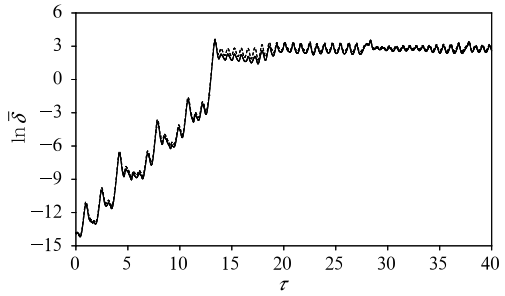

Fig. 10. As in Fig. 9, but for the other initial state $\boldsymbol{x}_{02}$(–7.28, –12.06, 16.15).

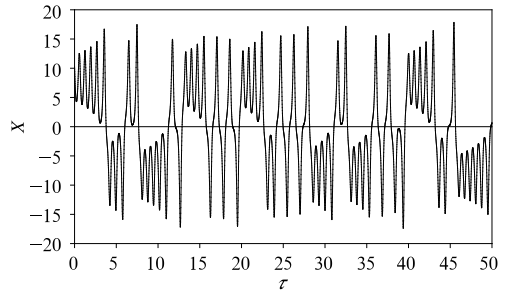

Fig. 11. Time evolution of the variable in the Lorenz system starting from the initial state $\boldsymbol{x}_{01}$(10.25, 6.33, 33.33).

When the magnitude of initial random error is reduced to 10^{-9} or increased to 10^{-1}, the AME and

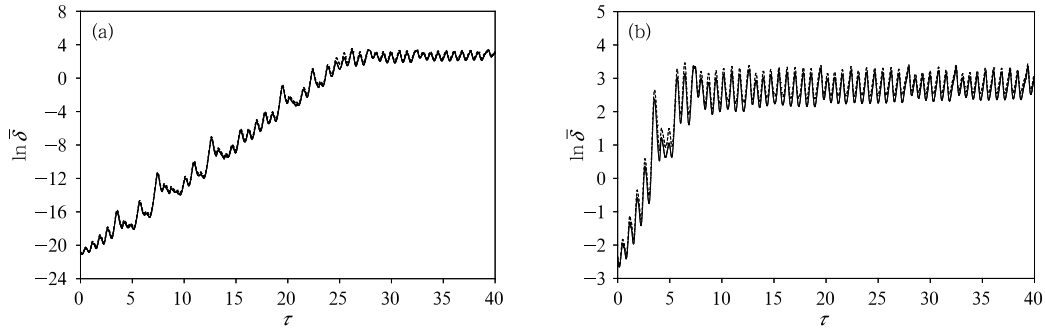

Fig. 12. As in Fig. 9, but the magnitudes of initial errors are (a) 10^{-9} and (b) 10^{-1}, respectively.

the GME also show consistent evolutions with time (Fig. 12). The curve of $\delta_0 = 10^{-6}$ (Fig. 9) seems to be a part of that corresponding to $\delta_0 = 10^{-9}$ (Fig. 12a). The results further demonstrate that the local dynamics of the unperturbed trajectory starting from an initial state determines the local error growth, which does not depend on the choices of the AME or the GME as a measure of the ensemble mean of error growth. The arithmetic mean can be used to investigate the local predictability of chaotic systems, and the geometric mean can do the same.

4. Summary and conclusions

To measure the global and local average predictability of chaotic systems, it is necessary to take the ensemble mean of error growth at different initial states over the chaotic attractor (or at the same initial state but with random errors of different directions). The methods of ensemble mean include the arithmetic mean and the geometric mean. In this paper, taking the Lorenz system as an example, we compare the influences of the arithmetic mean and the geometric mean on measuring the global and local average error growth. The results show that for the global average error growth, the GME shows a smoother growth than the AME. Because the growth rate of the AME shows a large fluctuation with time, if the growth rate of the error is used to measure the predictability, there would be a great uncertainty in the estimate of the predictability. But if the time at which error growth reaches saturation is defined as the limit of the predictability, the limits of the predictability obtained by using the AME and the GME are similar. During the phase of linear error growth, the exponential growth rate of the GME is equal to the maximal Lyapunov exponent, indicating that the GME is directly related to the maximal Lyapunov exponent. In contrast, the AME is unrelated to the maximal Lyapunov exponent. The saturation value of the AME represents the average distance between two points that are randomly chosen over the Lorenz attractor while the saturation value of the GME is related to the probability distribution of errors over the Lorenz attractor.

For the local average error growth, the error dynamics is dependent on the local dynamics of the unperturbed trajectory starting from the initial state. The evolutions of the AME and the GME are almost consistent, indicating that the choices of the AME or the GME have no influence on the measure of local average predictability. It should be pointed out that although the Lorenz's three-variable model (Lorenz, 1963) is relatively simple, it still provides us with some valuable information on the differences between the GME and the AME. A more complicated model, such as an atmospheric general circulation model (GCM), is more likely to be associated with a more complicated behavior. It is of practical significance to make a more thorough comparison of the error mean methods based on an atmospheric GCM instead of the Lorenz's three-variable model. This remains to be studied in the future.

REFERENCES

Dalcher, A., and E. Kalnay, 1987: Error growth and pre-

dictability in operational ECMWF forecasts. *Tellus*, **39A**, 474–491.

Ding, R. Q., and J. P. Li, 2007: Nonlinear finite-time Lyapunov exponent and predictability. *Phys. Lett. A*, **364**, 396–400.

——, ——, and K. J. Ha, 2008a: Trends and interdecadal changes of weather predictability during 1950s–1990s. *J. Geophys. Res.*, **113**, doi: 10.1029/2008JD010404.

——, ——, and ——, 2008b: Nonlinear local Lyapunov exponent and quantification of local predictability. *Chin. Phys. Lett.*, **25**, 1919–1922.

Eckmann, J. P., and D. Ruelle, 1985: Ergodic theory of chaos and strange attractors. *Rev. Mod. Phys.*, **57**, 617–656.

Gutiérrez, J. M., C. Primo, M. A. Rodríguez, et al., 2008: Spatiotemporal characterization of ensemble prediction systems the mean variance of the logarithms (MVL) diagram. *Nonlin. Processes Geophys.*, **15**, 109–114.

Krishnamurthy, V., 1993: A predictability study of Lorenz's 28-variable model as a dynamical system. *J. Atmos. Sci.*, **50**, 2215–2229.

Lang, X. M., and H. J. Wang, 2005: Seasonal differences of model predictability and the impact of SST in the Pacific. *Adv. Atmos. Sci.*, **22**, 103–113.

Legras, B., and M. Ghil, 1985: Persistent anomalies, blocking and variations in atmospheric predictability. *J. Atmos. Sci.*, **42**, 433–471.

Leith, C. E., 1983: Predictability in theory and practice. *Large-Scale Dynamics Processes in the Atmosphere.* Hoskins, B., and R. Pearce, Eds., Academic Press, New York, 391–405.

Li Jianping and Chou Jifan, 1997: Existence of atmosphere attractor. *Sci. China (Ser. D)*, **40**, 215–224.

—— and Wang Shouhong, 2008: Some mathematical and numerical issues in geophysical fluid dynamics and climate dynamics. *Commun. Comput. Phys.*, **3**, 759–793.

López, J. M., C. Primo, M. A. RodrÍguez, et al., 2004: Scaling properties of growing noninfinitesimal perturbations in space-time chaos. *Phys. Rev. E*, **70**, doi: 10.1103/PhysRevE.70.056224.

Lorenz, E. N., 1963: Deterministic nonperiodic flow. *J. Atmos. Sci.*, **20**, 130–141.

——, 1965: A study of the predictability of a 28-variable atmospheric model. *Tellus*, **3**, 321–333.

——, 1969: Atmospheric predictability as revealed by naturally occurring analogues. *J. Atmos. Sci.*, **26**, 636–646.

——, 1982: Atmospheric predictability experiments with a large numerical model. *Tellus*, **34**, 505–513.

Mu, M., W. S. Duan, and J. C. Wang, 2002: The predictability problems in numerical weather and climate prediction. *Adv. Atmos. Sci.*, **19**, 191–204.

Nese, J. M., 1989: Quantifying local predictability in phase space. *Physica D*, **35**, 237–250.

Palmer, T. N., F. Molteni, R. Mureau, et al., 1993: Ensemble prediction. *Seminar on Validation of Models over Europe*, Vol. 1, Shinfield Park, Reading, United Kingdom, ECMWF, 21–66.

Primo, C., M. A. Rodríguez, and J. M. Gutiérrez, 2008: Logarithmic bred vectors. A new ensemble method with adjustable spread and calibration time. *J. Geophys. Res.*, **113**, doi: 10.1029/2007JD008998.

Rose, C., and M. D. Smith, 2002: *Mathematical Statistics with Mathematica.* Springer-Verlag, New York, 221–230.

Simmons, A. J., R. Mureau, and T. Petroliagis, 1995: Error growth and estimates of predictability from the ECMWF forecasting system. *Quart. J. Roy. Meteor. Soc.*, **121**, 1739–1771.

Tracton, M. S., and E. Kalnay, 1993: Operational ensemble prediction at the National Meteorological Center: Practical aspects. *Wea. Forecasting*, **8**, 379–398.

Wolf, A., J. B. Swift, H. L. Swinney, et al., 1985: Determining Lyapunov exponents from a time series. *Physica D*, **16**, 285–317.

Yoden, S., and M. Nomura, 1993: Finite-time Lyapunov stability analysis and its application to atmospheric predictability. *J. Atmos. Sci.*, **50**, 1531–1543.

Zhou Xiuji, 2005: Atmospheric stochastic dynamics and predictability. *Acta Meteor. Sinica*, **63**, 806–811. (in Chinese)

Ziehmann, C., L. A. Smith, and J. Kurths, 2000: Localized Lyapunov exponents and the prediction of predictability. *Phys. Lett. A*, **4**, 237–251.